

P. Lalande, A. Delannoy †  
(Onera)

E-mail: philippe.lalande@onera.fr

# Numerical Methods for Zoning Computation

Zoning consists in establishing lightning strike zones to locate and classify surfaces on an aircraft which are exposed to a part of the lightning current components. The current standard used to certify aircraft is empirical and qualitative, and fails to predict certain features, such as lightning attachment on the middle of the wing. Furthermore, the standard will be difficult to apply to the next generation of aircraft having geometry, engines and fuselage material that will be very different from current designs. Two approaches have been developed to elaborate a zoning around an aircraft. An empirical developed by BAe is based on the rolling sphere model. The input parameter is the radius of the sphere which is evaluated by service lightning strike experience for a given aircraft. The second approach is based on the physical description of the lightning strike on an aircraft. From the physical modelling of lightning discharge, Onera has developed a general method to compute a probabilistic zoning. This method takes into account the fundamental processes occurring during a lightning strike on an aircraft. The attachment process is computed from the aircraft geometry and the atmospheric electric field direction leading to the lightning inception. The results of this computation give the initial points on the fuselage where a lightning can develop and their probability of inception as a function of the skin geometry and the field direction. These inputs are used in a swept model to compute, for each attachment point, the lightning attachment point displacement due to the aircraft motion, the airflow and the lightning channel geometry. The model is based, for computing power purposes, on a macroscopic description of the lightning channel during the continuous current phase. For a given single aisle aircraft, we compute and record in a database several million cases of lightning strikes. By using the distribution of lightning stroke arrival times, the probability that a specific zone of this aircraft will be struck by a stroke is computed.

## Introduction

A single-aisle aircraft is usually struck by lightning once a year. This event is unpredictable and unavoidable and can cause major safety issues if a specific protection design is not applied to the aircraft. This is why aircraft manufacturers have to demonstrate that their aircrafts are adequately protected from both the direct and indirect effects of lightning. The demonstration uses regulatory documents, such as Aerospace Recommended Practice (ARP) edited by the SAE international group, which explains how to proceed for the lightning certification. In the ARP 5412A [1], the lightning current waveforms are simplified by an idealised environment composed of a set of current waveforms A, B, C and D (figure 1). These waveforms are not

intended to copy a specific lightning event but to reproduce the same effects on the aircraft as those expected from natural lightning. The current waveforms A and B represent the effect of a first return stroke and the waveform D, the effect of a subsequent return stroke. The waveform C simulates the effect of continuing lightning current.

During a lightning strike on an aircraft not all of these current components enter and exit an aircraft at the same spot. The lightning channel can remain stuck to certain zones, like the wingtips, while the attachment point remains only for a limited time on other parts of the aircraft. The purpose of establishing lightning strike zones (Zoning computation) is to locate and classify surfaces on an aircraft which are exposed to a part of these four composite current components.

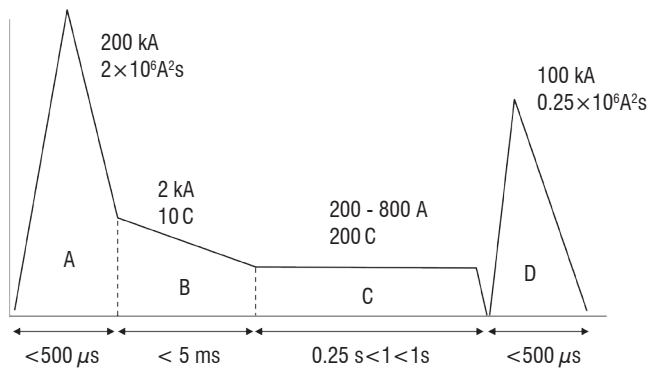


Figure 1 - Current components A, B, C, D for direct effects testing recommended in the ARP 5412A [1]

The zoning is the first step in protection design and the guidance for its implementation are described in the ARP5414A [2]. In the regulatory guide [2] the surface of the aircraft is divided into a set of regions called lightning strike zones. Three main zones, index 1, 2 and 3, are defined depending on whether the zone can experience a direct attachment of a lightning attachment point and whether the current flowing in the attachment point is due to a first or a subsequent return stroke. The previous zones are subdivided, A, B and C, to take account of duration while the attachment point remains hanging on to the zone. In the ARP5414A the six following zones are specified and the current threat associated with each zone is presented Table 1:

- zone 1A: First Return Stroke Zone with small Hang-On of the lightning attachment point
- zone 1B: First Return Stroke Zone with Long Hang-On of the lightning attachment point
- zone 1C: Transition Zone for the First Return Stroke with small Hang-On of the lightning attachment point
- zone 2A: Subsequent stroke with small Hang-On of the lightning attachment point
- zone 2B: Subsequent stroke with long Hang-On of the lightning attachment point.
- zone 3: Zone with no direct attachment of the attachment point on the zone and only subject to current conduction.

Zone	1	2
A	<p>200 kA <math>2 \times 10^6 A^2s</math></p> <p>A+B</p>	<p>D</p>
B	<p>A+B+C+D</p>	<p>D+C</p>
C	<p>100 kA <math>0.8 \times 10^6 A^2s</math></p> <p>Ah+B</p>	

Table 1 : Part of the lightning current waveforms set to each zone. For the zone C, a waveform  $A_h$ , between waveforms A and D, has been added.

The guidance in the ARP 5414 for the zoning of a new aircraft is neither based on mathematical rules nor physical methods but only on qualitative observations. An example of the zoning for transport aircraft, proposed by the ARP 5414A, is presented in figure 2. It is based on the similarity method. If a new aircraft has no significant differences compared to a previously certified aircraft the zoning of which has been validated by service lightning strike experience, then the same zoning can be used for both aircraft. No significant differences means no significant change in the electrical conductivity of the aircraft surface, no significant differences in the geometry, no significant changes in the flight characteristics (speed and altitude envelope). At the end of the zoning process, the zoning is reviewed with the certifying authority to obtain its concurrence.

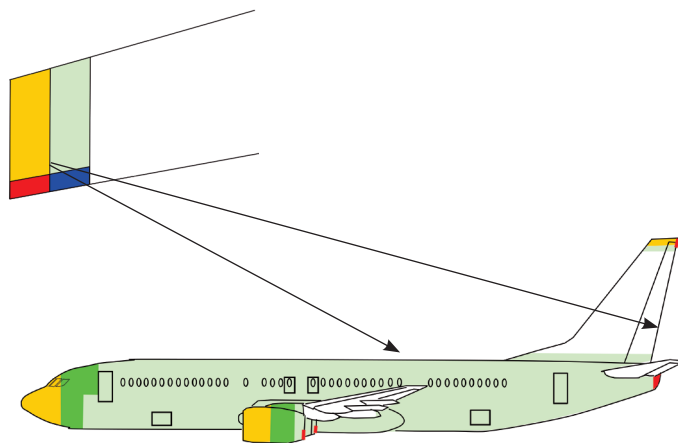


Figure 2 - Example of Lightning Strike Zone Details for Transport Aircraft [2]. The color scale is associated with the definition of zones 1 and 2. Zone 3 is white.

This approach, giving qualitative results, fails to predict damage due to lightning strikes at the middle of the wing such as observed in figure 3. No information is available on the type of lightning stroke (first or subsequent return stroke) associated with this damage. The zone surrounded by the black circle is usually considered in the ARP 5414A as a zone 3 where direct strikes of a lightning could not occur. Moreover, the guidance will be difficult to apply to the next generation of aircraft (figure 4) with both non conventional geometry and fuselage materials very different from aircraft currently in service.

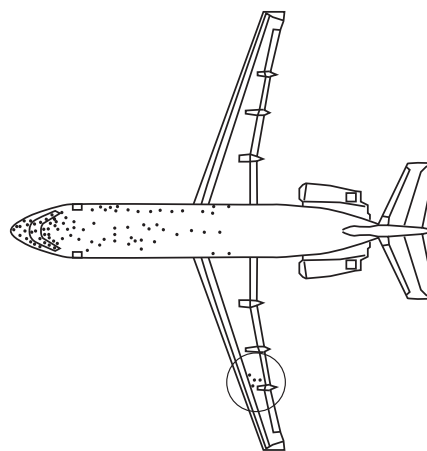


Figure 3 - Data collected by BAe in the framework of the European FULMEN project. The black dots on the fuselage show the lightning strikes to the aircraft. The circle surrounds the lightning strikes on the wing.

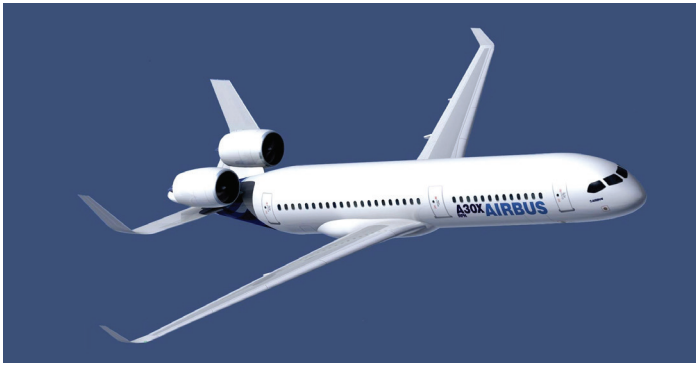


Figure 4 - A30X Concept for single-aisle aircraft [3]

The purpose of this paper is to review the numerical methods available for the zoning. Firstly, we review the different physical processes occurring during a lightning strike to aircraft. Secondly, we present and analyze the rolling sphere model used by British Aerospace (BAe) for the zoning [4]. Lastly, we present a new physical model for probabilistic zoning.

### Description of a lightning strike on an aircraft

In-flight lightning campaigns, detailed in Laroche et al. [5], have shown that in the majority of events it is the aircraft that triggered the lightning strike. The development of a lightning strike can be split into two elementary time sequences. The first, which lasts a few milliseconds, is associated with the inception and the development of the positive and the negative lightning leaders from the aircraft. The initiation points associated with the positive leaders are called entry points and exit points for the negative leaders. It determines the initial lightning attachment points. The process is so fast that the displacement of the aircraft can be ignored. The governing parameters for the location of the initial attachment points are the aircraft geometry, the fuselage materials and the electric field generated by the thundercloud. The second time sequence lasts several hundreds of milliseconds during which the lightning strokes strike the aircraft. The motion of the aircraft leads to the displacement of the two lightning attachment points on the fuselage, depending on their initial location. This phenomenon is called sweeping. It depends on the skin properties (paint thickness, rivets, junction, etc.), the aerodynamic flow profile, lightning channel characteristics and the initial location and orientation of the lightning channels connected to the fuselage.

### The rolling sphere model for the zoning

At the beginning of the twentieth-century, with the development of electricity, several research programs were run to reduce the effect of lightning on power transmission lines. By the 50's these studies had provided a rough mathematical description of the interaction between lightning and a grounded structure. This empirical model, called the electro-geometrical model [6], allows determination of the striking points (or attachment points). It only simulates the connection between a downward negative leader and a grounded structure. It should be remembered that the striking process results from the connection of the approaching negative leader and a positive upward "connecting leader" developing from the grounded structure. This positive leader initiates when the electric field due to the coming negative

leader reaches a minimum threshold. In this model the structure does not move so no sweeping is taken into account. It follows that the lightning channel remains hanging at the same spot during the lightning strike. In this case the initial attachment points and the striking points are the same which is not the case during lightning strikes on aircraft.

The determination of the attachment point (i.e. the point of inception of the positive connecting leader) is as follows:

- a sphere of radius  $R_\alpha$  is placed at the negative leader tip;
- the attachment point corresponds to the first point of the structure or of the ground which touches this sphere;
- the sphere, which is assimilated into "the attraction" zone of the negative leader, is rolled on all the structure surfaces (figure 5); all the points touched by the sphere can be struck by lightning.

We can see that the results depend to a great extent on the radius of the sphere  $R_\alpha$ . It is generally expressed, as a function of the peak current  $I$  of the first return stroke, by the following expression:

$$R_\alpha = aI^b \quad (1)$$

Where  $a$ ,  $b$  are some coefficients which are respectively in a range of [1-20] and [0.2-1], depending of the model used for the downward negative leader, and the inception threshold for the upward positive connecting leader [7].

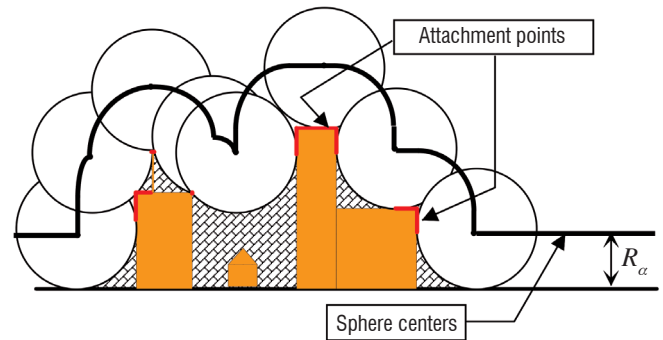


Figure 5 - Description of the rolling sphere method. The orange color represents buildings. The red lines represent the zones on the buildings which can be struck by lightning. The spheres are associated with the attraction zone of the negative downward leaders. The thick black line is associated with the sphere centers located at a distance  $R_\alpha$  from the ground or building surface. The crosshatched pattern is the zone where a lightning strike cannot occur.

BAe has applied the rolling sphere model to the case of a lightning strike on an aircraft to compute the initial attachment zones of the lightning [4] even if this model assumes that the aircraft intercepts natural lightning which is not consistent with in-flight observations showing that it is the aircraft which triggers the lightning strike.

The attachment points are computed by rolling the sphere on the aircraft surface (figure 6). The points touched by the sphere correspond to entry points. From the external surface generated by the sphere centers, the probability that an elementary surface of the aircraft may be struck can be inferred. For instance, in figure 6, the attractive zone of  $dS_1$  is the external surface  $S_1$  because all the negative leaders which enter the surface  $S_1$  are at the critical distance  $R_\alpha$  from  $dS_1$ . Then, all these leaders connect  $dS_1$ . The probability  $P_1$  associated with  $dS_1$  can be expressed as follows:

$$P = \frac{S_1}{S_{tot}} \quad (2)$$

where  $S_{tot}$  is the total external surface generated by the sphere centers.

This model always computes higher probability at the sharp extremity of the aircraft such as  $dS_1$  than at flat parts of the fuselage such as the surface at  $dS_2$ .

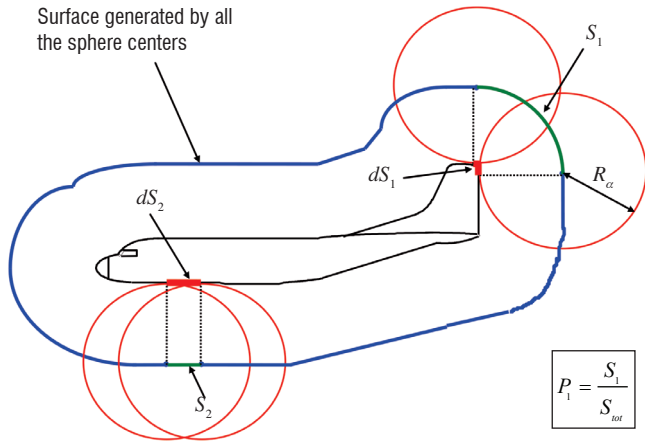


Figure 6 : Rolling sphere method applied to an aircraft.

The advantage of this model is to directly associate with a given area of the aircraft a probability of being struck by lightning. However, we have to remember that this method is based on an empirical model. It is consistent with one of the lightning strike processes which is the least probable in the case of aircraft. Moreover, the results greatly depend on the choice of the radius. It has been set by BAe in order that results are consistent with service lightning strike experience for a given aircraft. For a new aircraft, where the similitude approach could not be used, it will be difficult to determine the value of this parameter. Finally, the computation gives the initial attachment points and not the striking points where the damage is located. The sweeping process occurs between them and this is not taken into account in this model.

## Description of the physical approach for zoning design

Within the framework of European programs (FULMEN and EM-HAZ), Onera has adapted its physical models [8][9][10] simulating the development of lightning leaders to the processes occurring during a lightning strike on aircraft. Two models have been developed to be consistent with the observations [5]. The first, called the "attachment model", simulates the initial phase of a lightning strike on an aircraft. The second, called the "sweeping model", computes the displacement of the two lightning attachment points on the aircraft surface.

In this part, we present the main principles of these models, which are detailed in references [8][9][10][11][12][13][14], and we explain how they can be used and completed for a zoning approach.

### Attachment model

The attachment model is based on the electrostatic time-independent model described in [10], which is a simplification of the physical models [8][9]. The lightning leader is simulated by a space charge sur-

rounding the hot conductive plasma channel. Figure 7b illustrates this modeling in the case of an upward leader initiating from a grounded structure. The lightning leader can propagate until the potential drop  $\Delta U_T$  in front of the leader tip remains higher than 250 kV (figure 7a). The input parameters of this model are:

- the background atmospheric field  $E_o$ . It is assumed to be constant around and above the initiation structure;
- the space charge envelope radius  $a_{ce}$ ;
- the charge per unit of leader length  $q_{ce}$ .

Lalande et al. [10] set the parameters of  $q_{ce}$  to 50  $\mu\text{C}/\text{m}$  and  $a_{ce}$  to 0.5 m for a positive leader and to 140  $\mu\text{C}/\text{m}$  and 0.5 m for a negative leader in order that the results fit the ones derived from the physical models of Gallimberti et al. [9] and Bondiou et al. [8]. The physical models show that in order to take into account the effect of air density (altitude) on the leader development, the background electric field has to be divided by the reduced air density ( $\delta = P/P_o \cdot T_o/T$  where  $P$  and  $T$ ,  $P_o$  and  $T_o$  are the ambient air pressure and temperature and the standard pressure and temperature at Mean Sea Level, respectively). It means that a leader can develop in a lower atmospheric field at higher altitude than at mean sea level.

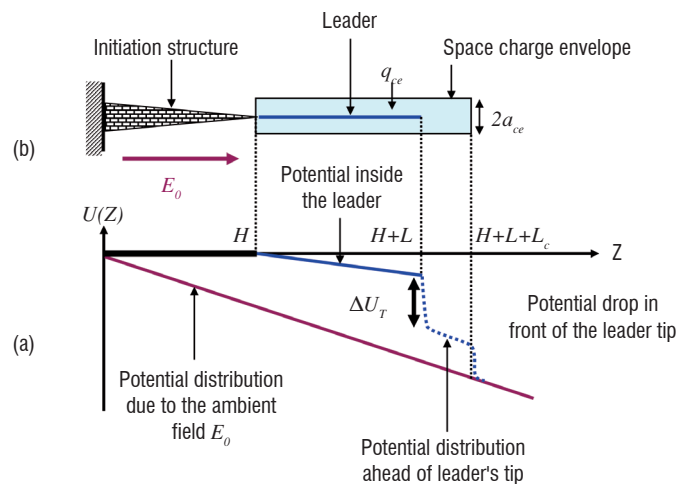


Figure 7 - Longitudinal potential distribution (a) along the path of an upward leader (b) developing from a ground structure.

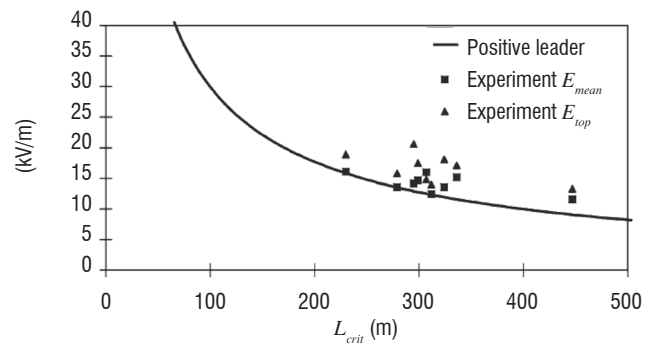


Figure 8 - Comparison between the computed stabilization field of a positive lightning leader (black line) and the measured mean atmospheric field  $E_{mean}$  (mean value of the atmospheric field along the rocket trajectory) just before the lightning is triggered [15].  $E_{top}$  is the atmospheric electric field at the altitude of the rocket tip (black triangle).  $L_{crit}$  is the length of spooled copper wire to trigger the lightning. It is similar to  $H$  in figure 7.

For a given geometry, we are able to compute from these models the minimum atmospheric field  $E_o$ , called the stabilization field, leading to a sustained propagation of the lightning leader from a structure. These



stabilization fields have been compared to the measurements of Willet et al. [15] in a case of rocket triggered lightning (figure 8). The good agreement between the measurements and the computation means we can apply this model to lightning strikes on aircraft.

In-flight lightning campaigns have shown that lightning strike starts from the development of a positive leader from the aircraft. The electrostatic set-up is the aircraft geometry and the direction of the background atmospheric electric field, generated by the thunderstorm. Electrostatic computations are made using a boundary element method (BEM, based on the solving of integral equations). From only one point "P", to minimize processing time, we compute, with the model described previously, the value of the stabilization  $E_{omin}$  (figure 9). We assume that points around the point "P" can also lead to lightning leader if the electric field on the aircraft skin is higher than the stability field inside a corona. For a positive corona, it is equal to 0.5 MV/m [16][17]. We prefer to use this rather than the air breakdown field (3 MV/m) because we are not able to take into account in the aircraft mesh all the sharp points due to dust, rivets, junctions, etc. which strongly enhance the surface electric field on the aircraft up to the air breakdown field (3 MV/m). At the end of this computation we shall have, for a given atmospheric field direction:

- the stabilization field  $E_{omin}$ ;
- an area where positive lightning leaders can develop.

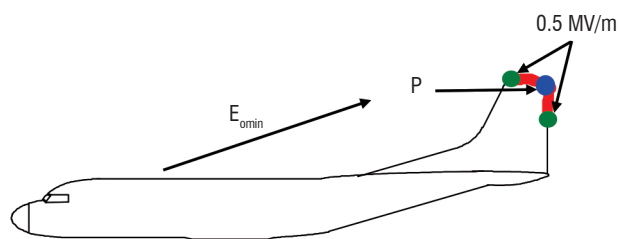


Figure 9 - Determination of the area of entry points (positive leader inception point) for a given direction of the ambient field.

The elongation of the positive leader from the aircraft increases the electric field at the opposite extremity of the aircraft. We compute for which positive leader length  $L_{min}$  a negative leader incepts from the point  $P'$  of the aircraft (figure 10). This length depends on the electric field  $E_{omin}$  and the aircraft size. We use the stability field of a negative corona (1 MV/m[18]) to define the area where a lightning negative leader can develop. Note that at this step the electric field on the fuselage is different to that of the previous step because of the presence of the positive leader.

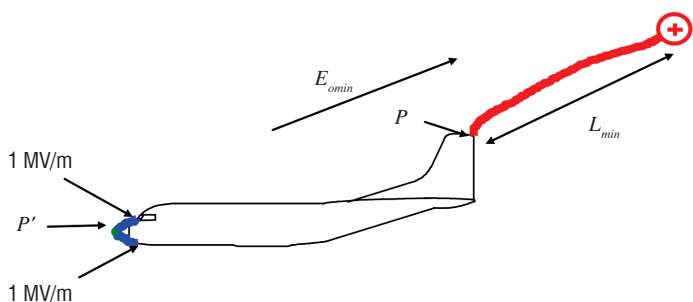


Figure 10 - Determination of the area of the exit points (negative leader inception point) for a given direction of the ambient field and length of the positive discharge.

From this model, two parameters have been computed for comparison to the in-flight lightning measurements taken with a Transall (C160) [19].

The first one is the stabilization field  $E_{omin}$ . The computed values, from 95 to 130 kV/m.Atm (depending on the angle between the atmospheric field direction and the fuselage), are in good agreement with the measured values which are in the range 84 to 124 kV/m.Atm. The second parameter available from the measurements is the time inception difference  $dTab$  between the positive and negative leaders. This parameter cannot be directly computed from the model which is a time independent model. We have only access to  $L_{min}$ . The mean value of  $L_{min}$  is 100 m. On the assumption that the positive leader velocity is between  $10^4$  and  $10^5$  m/s,  $dTab$  is in the range of 1 to 10 ms, which includes the measurements (table 2).

	Mesurements	Computation
$E_{omin}$ (kV/m/Atm)	$104 \pm 20$	95 to 130
$dTab$ (ms)	$4.3 \pm 2.7$	1 to 10 ms

Table 2: - Comparison between the measured and computed values of the stabilization field  $E_{omin}$  and the time inception difference between the positive and negative leaders.

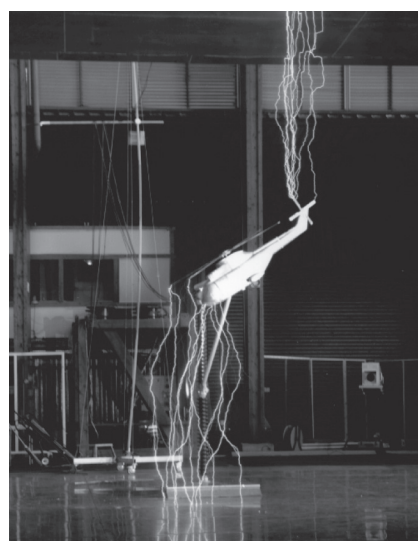


Figure 11 - Still photograph, taken at DGA-TA [20], of ten lightning strikes on a helicopter mock-up. The mock-up is electrically isolated from the ground and high voltage. It is placed inside a high voltage gap of 5 m composed of a planar electrode of 5x10 m above the ground.

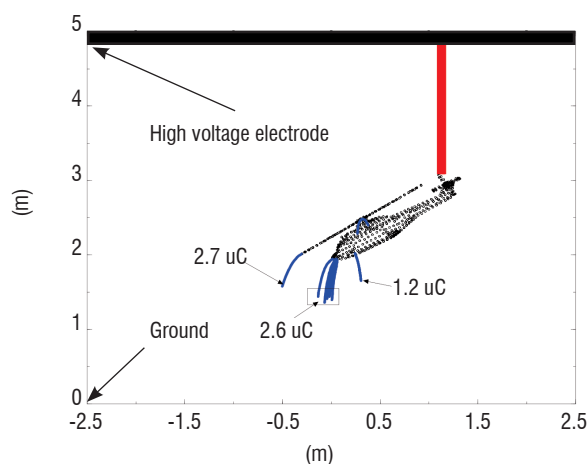


Figure 12 - Computation of the corona charge at some attachment points of the negative leaders for the test set-up of figure 11. The red line is associated with the positive leader and the blue lines the negative leaders. The electrostatic computation has been performed when the positive leader is connected the high voltage electrode.

At this step of the computation we have two zones associated with both leaders for a given atmospheric field direction and aircraft geometry. Inside a zone, the location the most probable for the leader inception is unknown. As part of the European FULMEN project, laboratory tests were performed at the DGA-TA test center [20] to simulate the inception of leaders from a mock-up [14]. The mock-up was placed above the ground and under a high voltage plane electrode. The mock-up was electrically isolated from the ground and the high voltage electrode. Figure 11 shows a still photograph of ten lightning strikes on a helicopter mock-up. We can see that, for a given set-up, multi-leader inception points are possible. An advanced analysis of these results has shown that the value of the corona charge, computed with the model of Goelian et al. [12], can be associated with the probability of a strike inside a given zone (figure 12). Where the charge is larger the probability of leader inception is higher.

On the aircraft surface mesh, the probability  $P_i$  that a positive leader initiates from the cell "i" of surface  $S_i$  is given by the following expression:

$$P_i = \frac{Q_i S_i}{\sum_{n=1}^N Q_n S_n} \quad (3)$$

where  $Q_j$  is the corona charge computed at the cell "j" and  $N$  is the total number of cells of the surface mesh.

We see that  $P_i$  varies with the direction of the background field.

### Sweeping model

The second model, called the Sweeping model, simulates the displacement of the lightning attachment point due to the motion of the aircraft. This model is described in detail in the articles of Larsson et al. [21][22]. Only the main principles are described here.

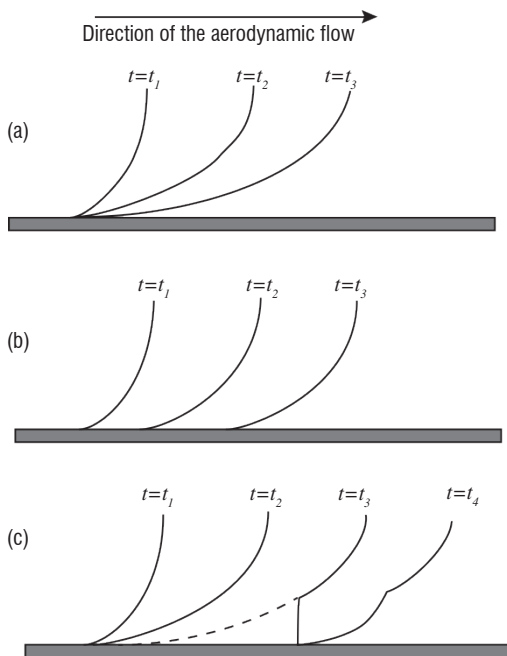


Figure 13 - Illustrations of three different swept-stroke phenomena. The lines represent the position of the lightning channel. (a) The attachment point remains at the same spot, (b) the attachment point sweeps continuously along the surface and (c) a breakdown occurs between the channel and the surface (at  $t=t_3$ ) and the attachment point makes a jump (a reattachment). The broken curve shows the short-circuited part of the channel [21].

Two phenomena may occur at the attachment point. Firstly, the attachment point may continuously sweep along the surface (figure 13b). Secondly, the attachment point may remain at the same spot (figure 13a) and thus follow the aircraft as it moves through the air. This results in a large deformation of the lightning channel until a reattachment (or re-connection) occurs (figure 13c).

A lightning channel has a more complex geometry and cannot be described by a simple line. The channel distortion is driven by magneto hydrodynamic forces which lead to a tortuous geometry of the channel and to its chaotic motion inside a tube of 10 to 15 cm of radius, as observed by Tanaka et al in the case of a long free burning arc [23] and Airbus France during lightning strikes on aircraft (figure 14).

In the model, the lightning channel is described by an equivalent tube of 30cm diameter that is drifted and distorted by the air flow. Larsson et al. [22] obtained consistent results with this model for the cases filmed during the in-flight lightning Transall Campaign.

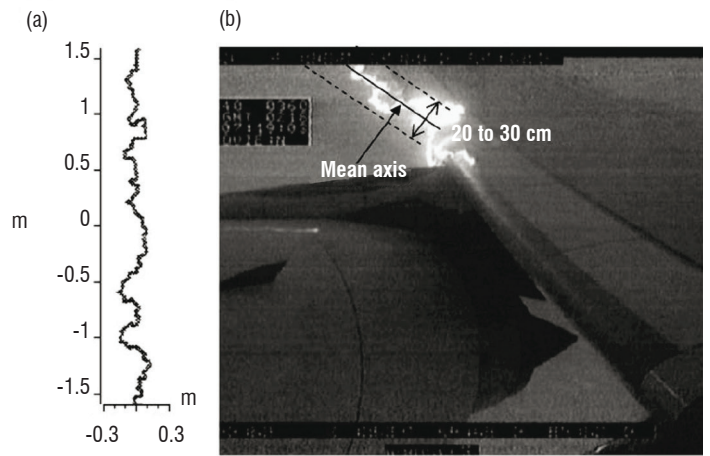


Figure 14 - Examples of a long free burning arc, (a) from Tanaka et al. [23], (b) from a lightning strike on an airliner (Photograph by Airbus France).

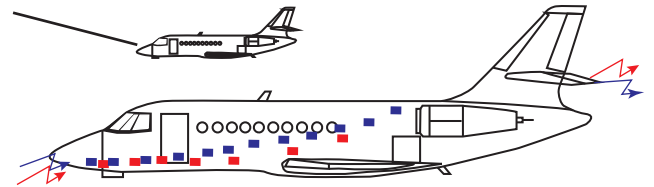


Figure 15 - Location of the lightning traces observed on the fuselage after two lightning strikes on a Falcon 2000; (blue dash) and (red dash). The grey line in front of the small aircraft shows the lightning channel location at the beginning of the sweeping.

Others comparisons have been performed by Broc et al. [24] with typical lightning strikes, collected by Dassault Aviation, on the Falcon Family. In a conventional case (figure 15), the lightning is initiated from the nose to the tail. The attachment points associated with the tail remain hanging on while the attachment points from the nose sweep along the fuselage following the stream lines of the air flow. The sweeping model has been applied to a Falcon 900 with an air flow configuration associated with an approach. In this configuration, the stream lines of air flow move back up along the fuselage. Only the lightning channel from the nose is considered. At the beginning of the computation it is assumed to be a straight line. The figure shows that the sweeping, assumed to be continuous, follows the stream lines

and the attachment point moves back up until a part of the lightning channel intercepts a stabilizer and jumps onto it.

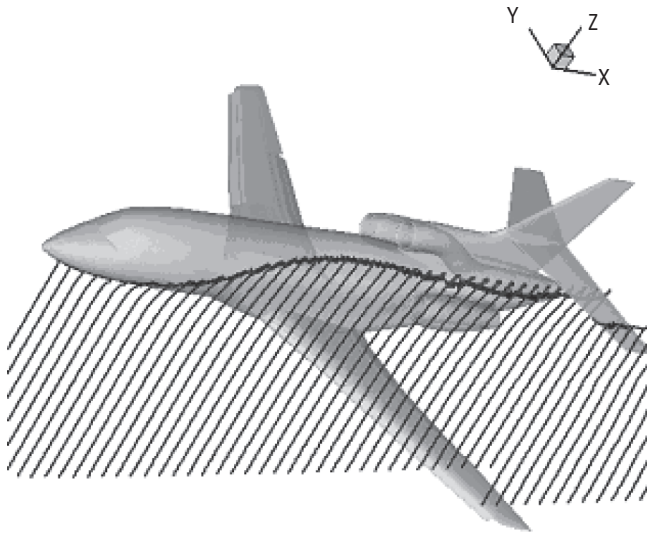


Figure 16 - Simulation of the sweeping of the lightning channels of the events shown in figure 15. The trace on the fuselage is the location of the attachment point. Each line corresponds to the lightning channel location at a given moment in time. In this case the air flow configuration is associated with an approach configuration (1000 ft,  $V = 130$  Kts,  $9.8^\circ$  angle of attack, flaps extended).

### Description of the probabilistic approach to zoning

From the both models previously described, we are able to build, for a given aircraft, a database of:

- for each thunderstorm field direction, the initial attachment points;
- for each attachment point, the sweeping trace on the fuselage and the location of the attachment point for a given moment in time.

Figure 17 presents data from the database for the case of a generic single-aisle aircraft. It is associated with a field direction  $E_0$  along the fuselage. The aircraft skin is assumed to be metallic with no paint layer leading to a continuous sweeping. The lightning channel (black line) is derived from the electric stream line from one of the initial attachment points. The sweeping model computes the time location of the attachment point from the initial attachment point. In this case, the attachment point sweeps from the nose to the wing root until the lightning channel intercepts the leading edge and the engine nacelle. Finally, the attachment point sweeps over the nacelle and remains hanging on at its extremity.



Figure 17 - Result of a sweeping starting from the initial attachment point and sweeping along the fuselage. The color scale represents the location in time of the attachment point on the fuselage. The computation has been performed on a generic single-aisle aircraft in cruise flight at a velocity of 250 m/s.

This approach has to be completed in order to determine all the locations of the damage associated with the lightning stroke components. The location of the damage will depend on the times of arrival of the lightning strokes. The figure 18 shows a typical lightning current composed of a continuing current on which three stroke currents, numbered 1, 2 and 3, have been superimposed. The location of the stroke damage on the aircraft (full white circles) are computed by using the time location of the attachment point (figure 17) and the time of arrival of each stroke.

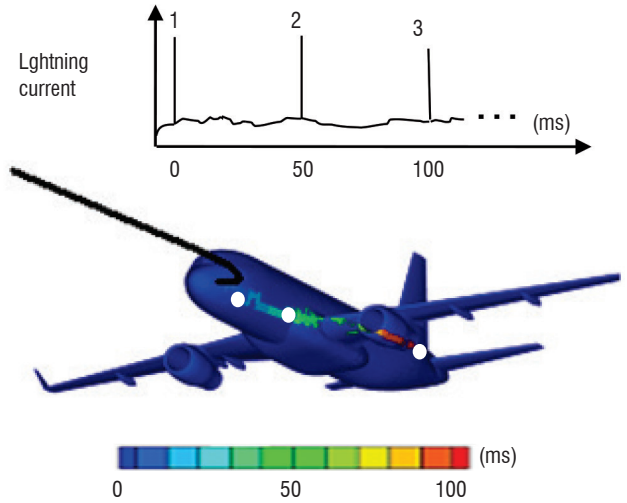


Figure 18 - Schematic figure of a typical lightning current composed of a continuing current on which three lightning strokes are superimposed. The full white circles show the lightning strikes due to the three strokes.

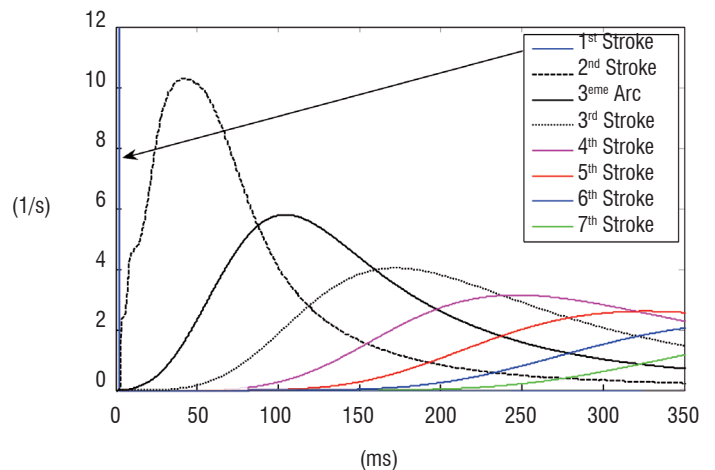


Figure 19 - Distributions of the time of arrival of strokes for a lightning strike on an aircraft at an altitude of 500 m. The distribution for the first stroke is not resolved in this figure. It is similar to a sharp peak.

The time of arrival of each lightning stroke is not deterministic. For each stroke (first, second, third, ...), the time of its arrival can be described by a statistic distribution that has been derived from both in-flight measurements and ground lightning network. It means, for instance, for the first stroke that the associated damages will not be located in a single point but distributed along the sweeping trace of figure 17 as a function of the time distribution of the first stroke arrival. At low flight altitude, the lightning strikes are due to cloud to ground lightning. Then, the time of arrival of the first stroke is the time for the lightning discharge to reach the ground (few milliseconds depending on the altitude). For the others strokes, the time of arrival is driven by the statistic distribution of the time between two strokes derived from observations. In figure 19, the



distribution of the time of arrival of the strokes has been plotted for a lightning strike on an aircraft at an altitude of 500 m.

The probabilistic approach of the zoning has to be completed by taking into account the distribution of the ambient field orientations experienced by the aircraft. In this article, an equi-distribution of the directions of thunderstorm fields is assumed.

The probabilistic zoning (figure 20) results in the combination of:

- The attachment/sweeping database which depends on the aircraft geometry and the flight parameters.
- The distribution of the time of arrival of lightning strikes.
- The distribution of the direction of the background atmospheric electric field associated with the thunderstorm.

## Results and discussion

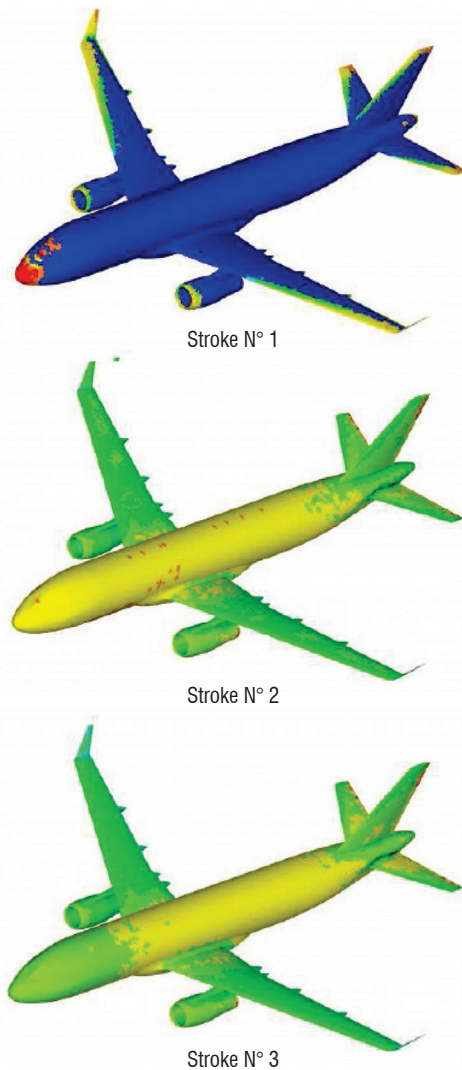


Figure 20 - Generic single-aisle aircraft flying at an altitude of 500m and a velocity of 250 m/s. The color scale is associated with probability value that a lightning stroke strikes a zone of the aircraft. It is a log scale probability from 10<sup>-3</sup> (red color) to 10<sup>-10</sup> (blue color).

Figure 20 shows a result of the probabilistic zoning associated with the geometry of a generic single-aisle aircraft flying at an altitude of 500 m and a velocity of 250 m/s. The surface mesh is composed

of 150,000 nodes and 300,000 triangles. 1800 field directions have been considered. For each direction, a mean value of 10,000 initial attachment points has been computed. All the results, corresponding to 18 million lightning strikes to this aircraft, have been stored in a dedicated database for this aircraft. Probabilistic zoning computes from this database the probabilities on this aircraft that a lightning strike hits a zone of the aircraft. In this figure, only the three first strokes have been presented. The color is on a log scale probability from 10<sup>-3</sup> (red) to 10<sup>-10</sup> (blue). Yellow is one decade higher than green. The first stroke is located near the initial points of attachment because the time for the lightning to reach the ground is 0.5 ms for an altitude of 500 m. The nose, the winglets and the extremity of the vertical stab are the zones where the probabilities are the highest. The probabilities are not zero on the leading edge but they are very small and strongly decreasing from the wing extremity to the wing root. The second stroke may occur between 1 ms to 150 ms (figure 19). During this period, the lightning attachment point has swept over the aircraft. The probabilities, mainly concentrated at the nose for the first stroke, spread over the fuselage, the wing and the nacelle for the second stroke. At the extremities of the stabs and trailing edge the probabilities increase due to the lightning attachment points which remain hung on. For the third stroke, the probability decreases at the front of the aircraft and increases at the rear because most of the attachment points have enough time to move from the front to the rear.

The probabilistic zoning is quite different from that derived from the ARP 5414A. Lightning strikes on the upper part of the wing are possible even if the probability is low. These lightning strikes are only due to subsequent strokes. This model based on lightning physics can be applied to any geometry (aircraft, launcher, helicopter, etc.) and could be introduced into a standard document to have a physical computation of the zoning.

## Conclusion

A new approach to zoning has been developed by Onera. It is based on two physical models. One simulates the lightning attachment processes on the aircraft. It computes the initial points of attachment of both lightning leaders (positive and negative). The second model simulates the sweeping processes of the lightning attachment point on the fuselage, from the initial attachment points until the attachment point remains hung on the fuselage. The output of this model is the time location of the attachment point on the fuselage which depends on the aircraft geometry, the air flow distribution and the lightning channel orientation. Both models are used to produce a database associated with a specific aircraft, holding all the possible points of initial lightning attachment and for each lightning attachment the associated sweeping points. From in-flight measurements and lightning ground networks, the statistic distribution of the time of arrival of each stroke has been determined. The probabilistic zoning is computed by combining the statistic distributions of time of arrival of each stroke with the background atmospheric field direction of the previous database. The results are probability values, on the aircraft surface, of being struck by one of the strokes. This new approach can be applied to the next generation of aircraft even if their geometry may be non conventional. Investigations shall have to be made to link this probabilistic zoning to standard zoning ■



## References

- [1] *Aircraft Lightning Environment and Related Test Waveforms*. ARP 5412A, 2005.
- [2] *Aircraft Lightning Zoning*. SAE ARP 5414A, 2005.
- [3] *Airbus' Global Market Forecast P82*. GMF, 2009.
- [4] C. C. R. JONES - *The Rolling Sphere as a Maximum Stress Predictor for Lightning Attachment and Current Transfer*. International Aerospace and Ground Conference on lightning and static electricity, Bath, 26-sept-1989.
- [5] P. LAROCHE, P. BLANCHET, A. DELANNOY, F. ISSAC - *Experimental Studies of Lightning Strike to Aircraft*. Aerospace Lab, 2012.
- [6] R. H. LEE - *Protection Zone for Buildings Against Lightning Strokes Using Transmission Line Protection Practice*. IEEE Transactions on Industry Applications, déc-1978.
- [7] R. H. GOLDE - *Lightning Volume 2 : Lightning Protection*. Academic Press. 1977.
- [8] A. BONDIOU, I. GALLIMBERTI - *Theoretical Modelling of the Development of the Positive Spark in Long Gaps*. Journal of Physics D: Applied Physics, vol. 27, no. 6, p. 1252-1266, juin 1994.
- [9] I. GALLIMBERTI, G. BACCHIEGA, A. BONDIOU-CLERGERIE, P. LALANDE - *Fundamental Processes in Long Air Gap Discharges*. Comptes Rendus Physique, vol. 3, no. 10, p. 1335-1359, déc. 2002.
- [10] P. LALANDE, A. BONDIOU-CLERGERIE, G. BACCHIEGA, I. GALLIMBERTI - *Observations and Modeling of Lightning Leaders*. Comptes Rendus Physique, vol. 3, no. 10, p. 1375-1392, déc. 2002.
- [11] A. DELANNOY, P. LALANDE, E. MONTREUIL, A. BROU, P. LAROCHE, F. UHLIG, V. SRITHAMMAVANH, S. ZEHAR, C. PROVENCHÈRE, H. ANDREU, C. ANDRÉ, H. W. ZAGLAUER, N. PEGG - *ATLAS: a Zoning Tool for Aircraft*. presented at the ICOLSE, 2003.
- [12] N. GOELIAN, P. LALANDE, A. BONDIOU-CLERGERIE, G. L. BACCHIEGA, A. GAZZANI, I. GALLIMBERTI - *A Simplified Model for the Simulation of Positive-Spark Development in Long Air Gaps*. Journal of Physics D: Applied Physics, vol. 30, no. 17, p. 2441-2452, sept. 1997.
- [13] P. LALANDE, A. BONDIOU-CLERGERIE, P. LAROCHE - *Computations of the Initial Discharge Initiation Zones on Aircraft and Helicopter*. presented at the ICOLSE, Toulouse, 1999.
- [14] P. LALANDE, A. BONDIOU-CLERGERIE, P. LAROCHE, A. ULMANN, P. DIMNET, J.-F. BOURILLON, L. TAMIN, A. DOUAY, F. UHLIG, P. GONDOT - *Determination in Laboratory of Zone of Initial Lightning Attachment on Aircraft and Helicopter*. presented at the ICOLSE, Toulouse, 1999.
- [15] J. . WILLET, D. . DAVIS, P. LAROCHE - *An Experimental Study of Positive Leaders Initiating Rocket-Triggered Lightning*. Atmospheric Research, vol. 51, no. 3-4, p. 189-219, juill. 1999.
- [16] C. T. PHELPS - *Field-Enhanced Propagation of Corona Streamers*. J. Geophys. Res., vol. 76, no. 24, p. PP. 5799-5806.
- [17] R. F. GRIFFITHS, C. T. PHELPS - *Positive Streamer System Intensification and its Possible Role in Lightning Initiation*. Journal of Atmospheric and Terrestrial Physics, vol. 36, no. 1, p. 103-111, janv. 1974.
- [18] *Negative Discharges in Long Air Gaps at Les Renardières, 1978 Results*. ELECTRA, 1981.
- [19] P. LALANDE, A. BONDIOU-CLERGERIE, P. LAROCHE - *Analysis of Available in-Flight Measurements of Lightning Strikes to Aircraft*. presented at the ICOLSE, Toulouse, 1999.
- [20] *DGA Techniques aéronautiques*. [Online]. Available: <http://www.defense.gouv.fr/dga/la-dga2/expertise-et-essais/dga-techniques-aeronautiques>. [Accessed: 29-mai-2012].
- [21] A. LARSSON, P. LALANDE, A. BONDIOU-CLERGERIE, A. DELANNOY - *The Lightning Swept Stroke Along an Aircraft in Flight. Part I: Thermodynamic and Electric Properties of Lightning Arc Channels*. J. Phys. D: Appl. Phys., vol. 33, no. 15, p. 1866-1875, août 2000.
- [22] A. LARSSON, P. LALANDE, A. BONDIOU-CLERGERIE - *The Lightning Swept Stroke Along an Aircraft in Flight. Part II: Numerical Simulations of the Complete Process*. J. Phys. D: Appl. Phys., vol. 33, no. 15, p. 1876-1883, août 2000.
- [23] S. TANAKA, S. KIN'YA, G. YUTAKA - *Three Dimensional Analysis of DC Free Arc Behaviour by Image Processing Technique*. Construction of Estimation Method of Column Path and Analysis of Long Gap Horizontal Free Arc Behaviour. Denryoku Chuo Kenkyujo Yokosuka Kenkyujo Hokoku, 1999.
- [24] A. BROU, P. LALANDE, E. MONTREUIL, J.-P. MOREAU, A. DELANNOY, A. LARSSON, P. LAROCHE - *A Lightning Swept Stroke Model: A Valuable Tool to Investigate the Lightning Strike to Aircraft*. Aerospace Science and Technology, vol. 10, no. 8, p. 700-708, déc. 2006.

## AUTHORS

---



**Philippe Lalande** graduated from the "Ecole Supérieure de Physique Chimie de Paris" Paris (1992) and received a PhD degree in Plasma Physics from University Paris XI (1996). He joined Onera in 1996 where he has been involved both in the modelling of lightning interaction with aircraft and in the development of onboard atmospheric sensors. He is the Head of the lightning and plasmas Research Unit at Onera Chatillon.



**Alain Delannoy** † (1951-2012) received a PhD in Atmospheric Physic from University PARIS 6 in 1979. He joined Onera in 1980 and was engaged in research on Atmospheric Electricity, Cloud microphysic and Physic of Lightning. His interest focused on in situ electrical measurements in cloud for what he setup specific instrumentations. He was engaged in lightning strike experiment on aircraft. Alain Delannoy was author and co-author of numerous articles and reports on Atmospheric Electricity and Lightning.